$\partial\sigma/\partial C$ and $\partial\sigma/\partial T$. Otherwise the experimental data may be noisy.

High-temperature heating of metal up to the boiling point, $T = T_b$, takes place in the central part of the weld pool surface in the overheating plateau region. As follows from physical considerations, $\gamma(T, C) \to 0$ at $T \to T_b$, independently of the oxygen content. This means that

$$\partial\sigma/\partial r = \beta_T \frac{\partial T}{\partial r} + \beta_C \frac{\partial C}{\partial r} > 0$$

within a certain temperature range ($T_{ext} < T < T_b$, where T_{ext} is the extreme temperature) below the boiling point, i.e. the surface tension coefficient at certain definite temperature $T = T_{ext}$ has a maximum, and direction of the surface force in this temperature range corresponds to the direct (from the centre to periphery of the pool) capillary convection. Therefore, the opposite, as well as direct (from the centre to periphery of the weld pool at $T \in [T_{ext}, T_b)$ and reverse (from the periphery of the weld pool to its centre at $T < T_{ext}$) capillary convections may simultaneously exist on the weld pool surface in A-TIG welding. In this case, two vortexes may form in the weld pool, the interaction of which results in the flow of the melt directed deep into the weld pool.

It should be noted in conclusion that, in our opinion, the available experimental data on dependencies $\beta_C = \beta_C(T, C)$ and $\beta_T = \beta_T(T, C)$ within a wide temperature range are insufficient to theoretically estimate with certainty the effect by the Marangoni convection on the penetrating capacity of A-TIG welding. Investigation of this effect requires additional experimental studies of the dependence of the surface tension coefficient on the temperature and concentration of an activating element in the melt, especially for the conditions of interaction of the flux layer with the weld pool surface.

1. Paton, B.E., Yushchenko, K.A., Kovalenko, D.V. et al. (2006) Role of quasi-keyhole and Marangoni convection in formation of deep penetration in A-TIG welding of stainless steel (Phenomenological model of A-TIG welding of stainless steel). In: *Proc. of Joint 16th Int. Conf. on Computer Technology in Welding and Manufacturing and 3rd Int. Conf. on Mathematical Modelling and Information Technologies in Welding and Related Processes* (Kiev, Ukraine, June 2006). Kiev: PWI, 258–263.
2. Yushchenko, K.A., Kovalenko, D.V., Kovalenko. I.V. et al. (2007) Phenomenological model of existence and interaction of the system of activated arc and liquid channel of metal pool in A-TIG welding. *IIW Doc. XII-212-1112–07*.
3. Yushchenko, K.A., Kovalenko, D.V., Krivtsun, I.V. et al. (2008) Experimental studies and mathematical modelling of penetration in TIG and A-TIG stationary arc welding of stainless steel. *IIW Doc. XII-212-1117–08*.
4. Yushchenko, K.A., Kovalenko, D.V., Kovalenko, I.V. (2003) Investigation of peculiarities of A-TIG welding of stainless steels. *IIW Doc. 212-1047–03*.
5. Lancaster, J.F., Mills, K.C. (1991) Recommendations for the avoidance of variable penetration in gas tungsten arc welding. *IIW Doc. 212-796–91*.
6. Taimatsu, M., Nogi, K., Ogino, K.J. (1992) Surface tension of liquid Fe–O alloy. *High Temp., Soc. Jap.*, 18(**1**), 14–19.

RISK OF FORMATION OF CARBIDES AND α-PHASE IN WELDING OF HIGH-ALLOY CHROME-NICKEL STEELS

V.I. MAKHNENKO[1], **S.S. KOZLITINA**[1], **L.I. DZYUBAK**[1] and **V.P. KRAVETS**[2]
[1]E.O. Paton Electric Welding Institute, NASU, Kiev, Ukraine
[2]Rivnenskaya NPP, Kuznetsovsk, Ukraine

The possibility is considered of using calculation methods to predict the risk of formation of the σ-phase in the HAZ metal of chrome-nickel steels at a carbon content of about 0.08 % and higher. It is shown that the use of temperature-time constitutional diagrams for steel of a corresponding composition, combined with temperature cycles at points in the HAZ metal, allows predicting the degree of sensitization of the corresponding HAZ region under different welding conditions.

Keywords: *arc welding, chrome-nickel steels, welded joints, sensitization, σ-phase, intergranular cracks, stress corrosion, temperature-time diagram*

Problem of formation of the third phases is one of the fundamental in welding of austenite chrome-nickel steels with increased content of carbon. Corresponding recommendations were developed for its solving and included in many reference books [1 and others]. It is characteristic that mentioned third phases (besides initial austenite and ferrite) appear after a primary crystallization during some soaking at specified temperature interval (Figure 1). They made no serious problems for the near-weld zone metal in a single run welding. An overlay of the curves of thermal cycles for specific points of the near-weld zone on respective temperature-time diagrams (*c*-curves) for steel of a corresponding composition (Figure 2) in multi run welding, however, shows that the accumulation of conditions for formation of the chromium carbides along the grain boundaries (due to diffusion of carbon controlled by *c*-curve in Figure 2, *a*) or σ-phase accumulation due to δ-ferrite decay and formation of complex intermetallics (Figure 2, *b*), also controlled by diffusion processes, occur in the near-weld zone. Avrami method [2, 3] with coefficients, determined depending on temperature and level of formation of

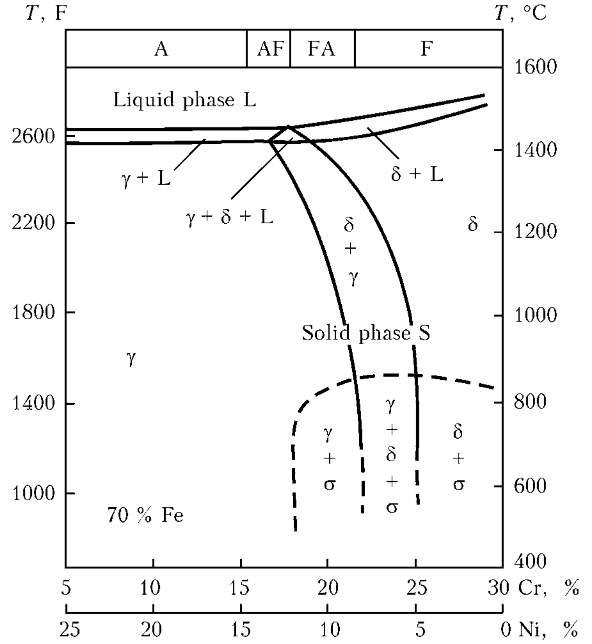

Figure 1. Phase constitutional diagram of Fe–Cr–Ni system at 70 % Fe [1]: A — austenite crystallization; AF — mainly austenite crystallization; FA — mainly ferrite crystallization; F — ferrite crystallization

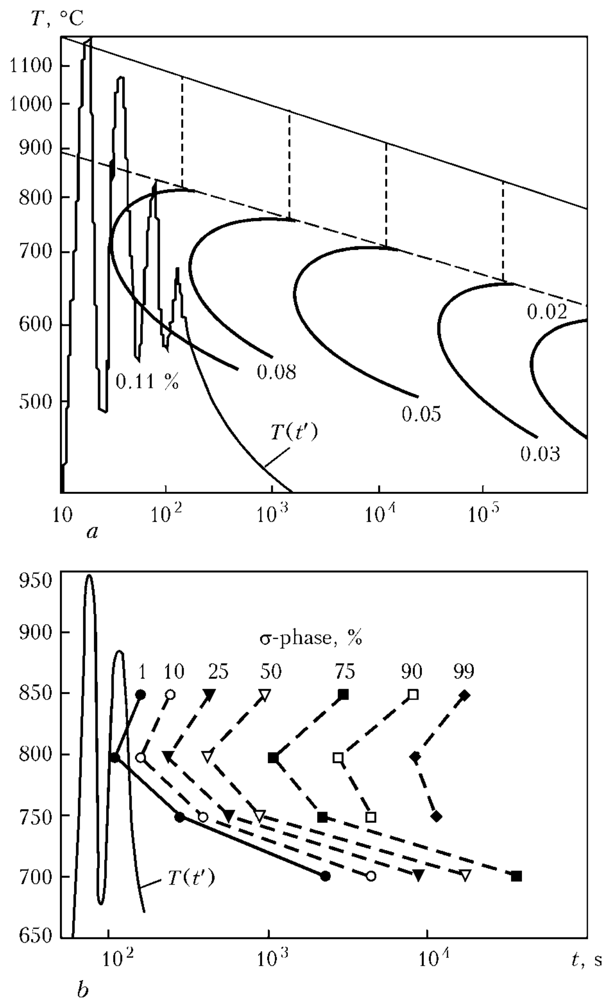

Figure 2. Temperature-time diagrams of formation of carbides in 18Cr9Ni type steel depending on content of carbon [1] (*a*) and σ-phase in DSS steel (22.4 Cr; 4.88 Ni; 3.13 Mo; 0.14 Mn; 0.67 Si; 0.18 N; 0.023 C) [2] (*b*)

new phase at given temperature in the case of very long soaking, was used in study [2] for description of the *c*-curves, related with σ-phase formation. Usage of given method is complicated by a wide spread in values of the corresponding coefficients for description of the *c*-shaped temperature-time curves of a type shown in Figure 2.

Present work proposes an approach based on a numerical integration of accumulation of effect of new phase presence in a specific point of the near-weld zone with given thermal cycle $T(t')$ based on data of corresponding *c*-shaped curve. A derivative $\partial T/\partial\tau$, proportionally to which indicated process of accumulation develops [4], can be calculated at any point of $T_{\min} < T < T_{\max}$ for it.

During formation of chemical compound (chromium carbides) (see Figure 2, *a*) the integration for an alloy with specific carbon content at $\partial T/\partial\tau \approx T/\tau$ gives

$$v_{\text{carb}} = \int\limits_{\tau(T_{\max})}^{\tau(T_{\min})} \bar{v}_{\text{carb}} \frac{dt'}{\tau(T)} \approx v_{\text{carb}}\chi, \tag{1}$$

where $\chi = \int\limits_{\tau(T_{\max})}^{\tau(T_{\min})} \frac{dt'}{\tau(T)}$ is the level of sensitization in the given point of HAZ with thermal cycle $T(t')$; v_{carb} is the carbide contents corresponding given *c*-shaped curve in Figure 2, *a*.

In case of the σ-phase, when intensity of the accumulation depends on temperature as well as level of already accumulated σ-phase (see Figure 2, *b*), the integration is carried out on each *c*-shaped curve, corresponding accumulated σ-phase, i.e.

$$v_\sigma = \sum_{j=1} \bar{v}_{\sigma j} \int\limits_{\tau(T_{\max})}^{\tau(T_{\min})} \frac{dt'}{\tau_j(T)}, \tag{2}$$

where $\bar{v}_{\sigma j}$ is the cost of *j*-th *c*-curve in Figure 2, *b*.

Two specific examples will be considered. 100 % monitoring of 1451 joints of Du 300 pipeline of the primary coolant circuit of multiple forced circulation was carried out on power block No.3 of Chernobylskaya NPP in a period of mid-life repair at the end of October, 1997. 208 joints among them had defects which were qualified as cracks of intercrystalline stress corrosion. Du 300 pipelines of 325 × 16 mm section were run from April, 1981, pipe material was steel 08Kh18N10T, joints were welded by 04Kh19N11M3 grade wire providing low (not less than 0.06 %) content of carbon in the weld metal.

Intercrystalline cracks were found in the HAZ metal (Figure 3) close to inner surface. A thermal cycle, related with welding in six runs (taking into account root run), according data of [5], is shown in Figure 4. Digitized *c*-shaped curve from the Table was used. The sensitization level according to data of Figure 4

Temperature-dependent values of $\tau(T)$ for different carbon content

T, °C	C = 0.11 %	C = 0.08 %
540	754.6	–
550	635.5	–
560	546.3	1000.0
570	419.8	894.1
580	300.8	793.5
590	233.9	719.4
600	122.3	629.4
610	85.5	555.3
620	79.6	502.4
630	73.6	444.1
640	67.7	401.8
650	62.5	364.7
660	58.0	338.7
670	53.6	327.6
680	48.3	306.5
690	46.1	327.6
700	44.6	343.5
710	43.1	375.3
720	45.4	417.6
730	47.6	470.6
740	50.6	613.5
750	55.0	931.2
760	58.0	1158.8
770	64.7	–
780	71.4	–
790	85.5	–
800	94.5	–

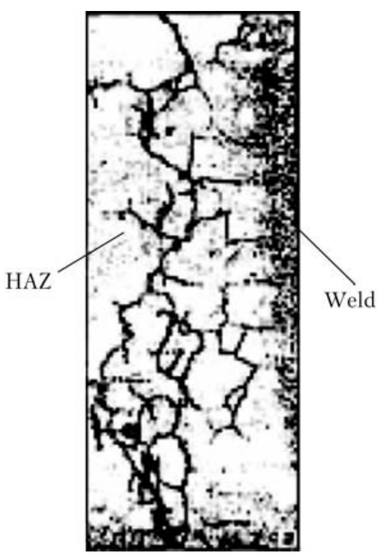

Figure 3. Microstructure (reduced 3/4) of circumferential operating cracks in the near-weld zone of Du 300 welded joint

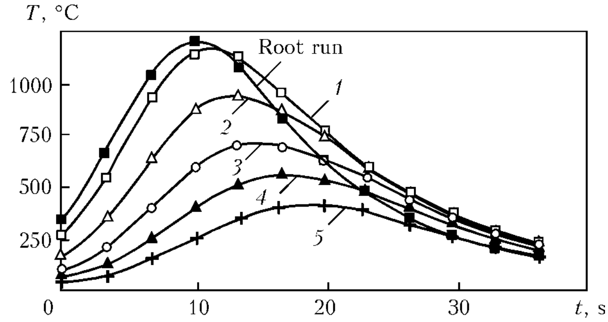

Figure 4. Temperature cycles on the inner surface at root run and next ones (*1–5*)

depending on run is the following: root run — 0.0085; 1st — 0.0529; 2nd — 0.0536; 3rd — 0.0306; 4–5th — 0. It is seen from these data that $\chi_\Sigma \approx 0.15$, i.e. noticeable enough level of sensitization of regions of the HAZ metal on the inner surface of pipe is present, that promoted nucleation and development of damages — cracks of intercrystalline stress corrosion, taking into account additional factors (stressed state in the HAZ metal on the inner surface of pipe and presence of corrosion medium — water of the primary coolant circuit at temperature around 280 °C). It is shown in series of works, for example [5], that the fracture toughness of the HAZ metal of 08Kh18N10T steel is at the level of 65 MPa·m$^{1/2}$ in the region of studied joints of Du 300, i.e. significantly lower of that behind the HAZ limits, where sensitization is absent.

Let us consider one more example. In 2009 in block No.2 of Rivnenskaya NPP a leak had appeared in a zone of connecting the pipeline and Du 250 T-bend (Figure 5) on Du 90 branch 273 × 20 mm of the pipeline of the primary coolant circuit. The pipeline material was steel 08Kh18N10T.

Crack-like through defect of around 150 mm length was found by means of non-destructive testing on the inner surface along the HAZ of circumferential weld with escaping on the outer surface in a form of circumferential crack (around 10 mm) of significantly smaller length. Beginning of the crack on the inner surface and ending on the outer have various axial coordinates, differing by 20–30 mm, i.e. the crack propagated not normal to pipe axis, but in a plain at an angle of 45° to this axis. If assume that found defect is the crack of intercrystalline stress corrosion, then a place of its nucleation is sensitized region of the

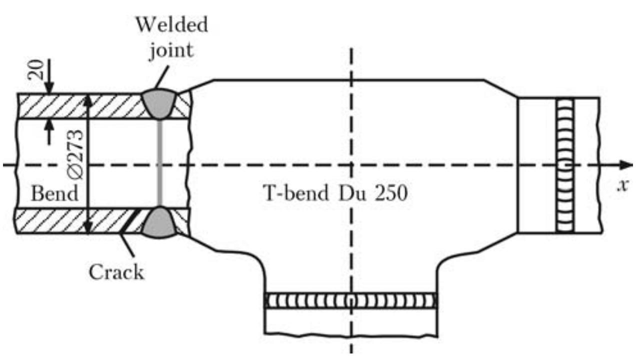

Figure 5. Scheme of a crack in welded joint with T-bend

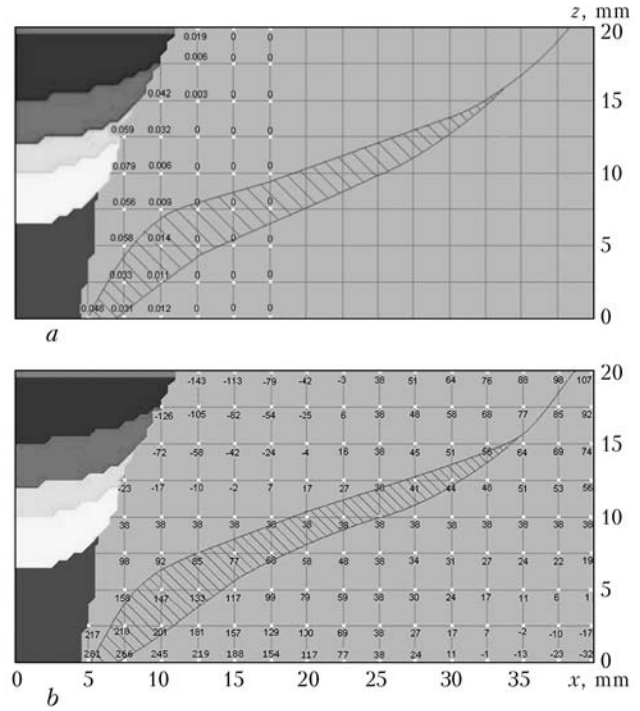

Figure 6. Possible trajectory of crack of intercrystalline stress corrosion and calculated values of χ_Σ in six run welding of butt weld (δ = 20 mm, steel 08Kh18N10T) (*a*) and transverse stresses σ_{zz} [MPa] (*b*)

HAZ on the inner surface (Figure 6, *a*) resulted from multirun (6–7 runs) effect of the thermal cycles according to types given in Figure 4. The crack propagated during a long period of time (block was implemented in 1981) under the effect of axial stresses σ_{xx} from internal pressure in the pipe:

$$\sigma_{xx}(P) = P\,\frac{R/\delta}{(2+\delta/R)}, \qquad (3)$$

and residual welding stresses [6]:

$$\sigma^{w}_{xx} \approx -\sigma_0\left[\cos\frac{\pi x}{2x_1}\right]\frac{2z}{\delta}$$
$$\text{at } 0 < x < x_1,\ -\delta/2 < z < \delta/2,$$
$$\sigma^{w}_{xx} \approx -\sigma_2\left[\sin\frac{\pi(x-x_1)}{2(x_2-x_1)}\right]\frac{2z}{\delta} \qquad (4)$$
$$\text{at } x_1 \le x < x_2,\ -\delta/2 < z < \delta/2,$$

where R is the inner radius of the pipe.

Approximate dependences (4), describing results of numerical calculations for circumferential welded joints of pipe on austenite steel, were built on data of [6]. Distribution parameters σ_0, σ_2, y_1, y_2 depending on $\sqrt{R\delta}$, $q_{\rm h.i}/\delta$ and $\sigma_{\rm y}$ are given in [6], i.e. for

$$R = \frac{243}{2} - 20 = 116.5 \text{ mm},\ \sqrt{R\delta} = 48.3 \text{ mm},$$
$$q_{\rm h.i} \approx 8372 \text{ J/cm}^2,\ \sigma_{\rm y} = 300 \text{ MPa}$$

gives

$$\sigma_0 = 270 \text{ MPa},\ \sigma_2 = -75 \text{ MPa},\ y_1 \approx 30 \text{ mm},\ y_2 = 75 \text{ mm}.$$

Corresponding results of calculation of sum $\sigma_{xx}(P) + \sigma^{w}_{xx} = \sigma_{xx}$ in different points (z, x) on wall of the pipe in the zone of welded joint are given in Figure 6, *b*. It can be seen from these data that a trajectory of found crack-like defect is a result of compromises between the high values of χ_Σ of material sensitization in the HAZ and tensile stresses σ_{xx} that allows considering intercrystalline stress corrosion to be a mechanism of nucleation and propagation of found defect.

Setting of a sealing coupling in the zone of indicated through defect, with which a pressure in defect zone to be similar on inner and outer pipe surfaces (between the walls of pipe and coupling), allowed rapid reduction of a risk of spontaneous defect growth. This gave the possibility to set in operation the block No.2 of Rivnenskaya NPP at the height of winter campaign of 2009 up to forthcoming middle-life repair in 2010.

CONCLUSIONS

1. It is possible enough to obtain a high level of metal sensitization, related with sensitivity to intercrystalline stress corrosion as well as metal embrittlement in the HAZ, in the near-weld zone in welding of austenite steels with a carbon content of 0.08 % and higher.

2. Application of time-temperature diagrams of formation of carbides and σ-phase for austenite steels of corresponding composition allows predicting the level of sensitization of metal according to specific thermal cycle that develops additional possibility for control of structure and properties in the HAZ metal.

1. (1998) *Welding handbook. Materials and applications*. Pt 2. Miami: AWS.
2. Elter, J.W., Palmer, T.A., Specht, E.D. (2006) Synchrotron based observations of sigma phase formation and dissolution in DSS. Ed. by H. Cerjak. In: *Mathematical modeling of weld phenomena*, 297–315.
3. Hell, E.O., Alqie, S.H. (1966) The sigma phase. *Metallurgical Rev.*, **11**, 61–68.
4. (1986) *Metallurgy and technology of welding of titanium and its alloys*. Ed. by V.N. Zamkov. Kiev: Naukova Dumka.
5. Zubchenko, A.S., Kharina, I.L., Runov, A.E. et al. (2000) Corrosion-mechanical strength of welded piping of austenitic steels of RBMK reactors. *The Paton Welding J.*, **9/10**, 45–53.
6. Makhnenko, V.I. (2006) *Safety service life of welded joints and assemblies of current structures*. Kiev: Naukova Dumka.